Desalination and Water Treatment
www.deswater.com
16 (2010) 271–281
April
1944-3994/1944-3986 © 2010 Desalination Publications. All rights reserved
doi: 10.5004/dwt.2010.1058

Comparative study on the removal of zinc(II) by bovine bone, billy goat bone and synthetic hydroxyapatite

S. Meski[a,*], H. Khireddine[a], S. Ziani[a], S. Rengaraj[b,*], Mika Sillanpää[b]

[a]*Faculté de Technologie, Département de Génie des Procédés, Laboratoire de Génie de l'Environnement, Université de Bejaia, Algérie email: meskisamira@yahoo.fr*
[b]*Laboratory of Applied Environmental Chemistry (LAEC), Department of Environmental Science, University of Eastern Finland, Patteristonkatu 1, FI-50100 Mikkeli, Finland*
Tel. +358 (40) 355 3705; Fax: +358 (15) 355 6513; email: srengaraj1971@yahoo.com

Received 4 October 2009; Accepted 25 November 2009

ABSTRACT

The objective of this work is to investigate the possibility of using a low cost and naturally available apatite rich adsorbents from animal bones such as bovine bone (BV) and billy goat (BG) bones for the removal of zinc(II) from aqueous solutions. The adsorption studies were compared with synthetic hydroxyapatite (HAPs). The samples were characterized by thermogravimetry (TG), Fourier transform infrared spectroscopy (IR) and X-ray diffraction (XRD). The equilibrium isotherm data were fitted to the Langmuir, Freundlich, Temkin, Elovich and Dubinin-Redushkevich isotherm equations to obtain the characteristic parameters of each model. The adsorption of Zn(II) on BV and BG fitted well with the Langmuir isotherm where as HAPs fitted well with Dubinin Raduskevich isotherm model. The kinetic studies showed that the sorption rates could be described well by a pseudo-second-order kinetic model. Also it was shown that the adsorption of Zn(II) could be fitted to the intraparticle mass-transfer model. The studies showed that BG, BV and HAPs can be used as an efficient adsorbent material for the treatment of Zn(II) from water and wastewater. The order of the removal capacity for these adsorbents was determined as HAPs (93%) > BG (90%) > BV (82%).

Keywords: Adsorption; Animal bones; Hydroxyapatite; Isotherms; Kinetics; Zinc(II)

1. Introduction

Heavy metals such as lead, copper, zinc, cadmium and nickel are the most toxic pollutants present in marine, ground, and industrial wastewaters. In addition to their toxicity effects even at low concentrations, heavy metals can accumulate throughout the food chain, which leads to serious ecological and health hazards as a result of their solubility and mobility [1–3].

Zinc is one of the toxic heavy metal. In the Dangerous Substances Directive of the European Union (76/464/EEC), zinc has been registered as List 2 Dangerous Substance with Environmental Quality Standards being set at 40 μg/L for estuaries and marine waters and at 45–500 μg/L for freshwater depending on water hardness [4]. Zinc is commonly found in effluents discharged from ore processing after mining, acid mine drainage, galvanizing plants and municipal wastewater treatment plants. Zinc(II) is not biodegradable and is elevated through the food chain via bioaccumulation, therefore there is significant interest regarding its removal from wastewaters [5].

Various technologies exist for the removal of such metals, which include filtration, chemical precipitation, ion exchange, adsorption using activated carbon,

*Corresponding authors.

electrodeposition and membrane process [6–16]. All these methods are generally expensive [17]. Recently, Gupta *et al.*, [18–22] reviewed a wide variety of low-cost adsorbents for the removal of heavy metals. A low-cost adsorbent is defined as one that is abundant in nature, or is a by-product or waste material from another industry. Animal bone is an abundant natural waste product by slaughterhouse processing with millions of tons being generated annually. It has been proposed as a potential biosorbent with extensive studies having been carried out [23–24].

Animal bones contain 65–70% of inorganic substances, mainly hydroxyapatite ($Ca_{10}(PO_4)_6(OH)_2$). The remaining part of bones is composed of organic matter, mainly fibrous protein collagen [25].

Hydroxyapatite ($Ca_{10}(PO_4)_6(OH)_2$, HAP) is a member of apatite mineral family. It is an ideal material for long term containments because of its high sorption capacity for heavy metals, low water solubility, high stability under reducing and oxidizing conditions, availability and low cost [26]. There are many reports on using HAPs for the removal of heavy metals such as Co, Pb, Cu, Zn, Cd, Sb and Cr [26–28]. The mechanisms of the metal cations retention are different and include: ion exchange, adsorption, dissolution/precipitation, and formation of surface complexes [29,30].

The aim of this paper is to assess the ability of low-cost adsorbents such as bovine and billy goat bones to adsorb Zn(II) from aqueous solution and the results were compared with synthetic HAPs by conducting kinetics and different isotherm studies. The effect of the solution pH, contact time, initial Zn(II) concentration and adsorbent dosage on the removal of Zn(II) was also studied.

2. Materials and methods

2.1. Materials

All the reagents used were of analytical grade chemicals. A stock solution of zinc ions were prepared by dissolving appropriate amount of $ZnSO_4.7H_2O$ (Aldrich Chemical Company, USA) in double distilled water.

2.2. Preparation of the adsorbent

The bone samples (Billy goat and bovine bone) were cut into small pieces, and boiled in distilled water for 8 h for easy removal of the bone marrow and tendons. The bone samples were dried at 80°C for 24 h and sieved into particles sizes of $d_p \leq 0.335$ mm.

The synthetic hydroxyapatite powder was prepared by precipitation method using $Ca(NO_3)_2.4H_2O$ (98% purity) and $(NH_4)_2HPO_4$ (99% purity) and the pH of the solutions were adjusted with ammonia solution. The mole ratio of $Ca(NO_3)_2$ to $(NH_4)_2HPO_4$ was maintained at 1.67.

A suspension of 0.1 M $Ca(NO_3)_2.4H_2O$ was vigorously stirred and maintained at the room temperature. A solution of 0.06 mole $(NH_4)_2HPO_4$ was slowly added to the solution of $Ca(NO_3)_2.4H_2O$ solution. In all experiments the pH of $Ca(NO_3)_2.4H_2O$ solution was adjusted to pH 11 using ammoniac solution and the reactor was placed in an azote atmosphere under dynamic flow in order to prevent CO_2, which could result in carbonate apatite formation. This can be explained by the following reaction:

$$10Ca(NO_3)_2.4H_2O + 6(NH_4)_2HPO_4 + 8NH_4OH \rightarrow Ca_{10}(PO_4)_6(OH)_2 + 20NH_4NO_3 + 20H_2O. \quad (1)$$

The resulting powders were calcined at 600°C, to remove all organic matters. The obtained powders were named as BV (bovine bone), BG (billy goat) and HAPs (synthetic hydroxyapatite).

2.3. Characterization of the adsorbents

Thermogravimetric (TGA) analyses were carried out using thermogravimetric analyzer (Setaram TG-DTA92) in order to find out the calcination temperature. To study the crystallinity of the prepared samples, powder X-ray diffraction (XRD model PHILLIPS X pert proof, analytical, system MPD) patterns were recorded using CuKα radiation at 50 kV and 100 mA. Fourier transform infrared (FTIR model Shimadzu-8300) analysis was performed to identify the presence of functional groups in the samples. The adsorption capacities of Zn(II) were measured by using atomic absorption spectrometer with flame atomization (Shimadzu AA 6500, air/C_2H_5 gas mixture) for zinc content.

2.4. Batch mode adsorption studies

The stock solution was diluted as required to obtain standard solutions containing 10 to 100 mg/L of Zn(II). Two hundred milliliters of Zn(II) solution of a desired concentration, adjusted to a desired pH, was taken in reaction bottles of 400 mL capacity and known amounts of adsorbents were added. The solution pH was adjusted by using 0.1 N sulphuric acid or dilute potassium hydroxide solutions. The solutions were agitated for a predetermined period at 20 ± 1°C in a shaking incubator. The adsorbents were separated and the filtrate was analyzed by an atomic absorption spectrometer with flame atomization (Shimadzu AA 6500, air/C_2H_5 gas mixture) for zinc content.

2.5. Adsorption isotherm

Adsorption isotherm studies were carried out with 200 mL of different initial Zn(II) concentrations while

maintaining the adsorbent dosage at constant level. The equilibrium adsorption capacity was calculated using

$$q_e = \frac{(C_0 - C_e)^* V}{m}, \quad (2)$$

where q_e (mg/g) is the equilibrium adsorption capacity, C_0 and C_e the initial and equilibrium concentration (mg/L) of zinc ions in solution, V (L) the volume, and m (g) is the weight of the adsorbent.

2.6. Adsorption kinetics

Kinetic experiments were carried out by using a known weight of adsorbent and employing Zn(II) concentration in the range of 10–100 mg/L. The samples at different time intervals (0–240 min) were taken and filtered. Suitable aliquots were analyzed for Zn(II) concentration and recorded. The rate constants were calculated by using the conventional rate expression. The amount of metal ion sorbed q_t was calculated from

$$q_t = \frac{(C_0 - C_t)^* V}{m}, \quad (3)$$

where q_t (mg/g) is the adsorption capacity, C_0 and C_t are the initial and equilibrium concentration (mg/L) of zinc ions in solution, V (L) is the volume, and m (g) is the weight of the adsorbent.

2.7. Error analysis for isotherm studies

In the single component isotherm studies, the optimization procedure requires an error function to be defined in order to be able to evaluate the fit of the isotherm to the experimental equilibrium data. In this study, two different error functions were examined, and in each case, the isotherm parameters were determined by minimizing the respective error function across the concentration range studied. The error functions studied were as follows.

2.7.1. Marquardt's percent standard deviation (MPSD)

This error function was used previously by a number of researchers in the field [31]. It is similar to a geometric mean error distribution that has been modified to allow for the number of degrees of freedom in the system:

$$MPSD(\%) = 100 * \sqrt{\frac{\sum_{i,N} \left((q_{\exp i} - q_{cali}) / q_{\exp i} \right)^2}{N - 1}}. \quad (4)$$

2.7.2. The average relative error (ARE)

This error function attempts to minimize the fractional error distribution across the entire concentration range [31]:

$$ARE(\%) = \frac{\sum_{i=1}^{N} \left| \left((q_e)_{\exp i} - (q_e)_{\text{cali}} \right) \Big/ (q_e)_{\text{espi}} \right|}{N} * 100. \quad (5)$$

3. Results and discussion

3.1. Characterization of the materials

3.1.1. TG/ DTG analysis of BV, BG and HAPs

The TG and DTG patterns of bovine bone, billy goat bone and synthetic hydroxyapatite are shown in Fig. 1. The TG/DTG results of BV and BG shows two peaks at ~110 and ~350°C and synthetic hydroxyapatite shows only one peak at ~110°C. The first peak corresponds to physically adsorbed water, and the second is burning of organic samples. Two sequential processes, that is loss of water molecules by desorption of physically adsorbed water (110°C) and burning of organic substances (200–500°C) occurred. For bovine and billy goat bone, there

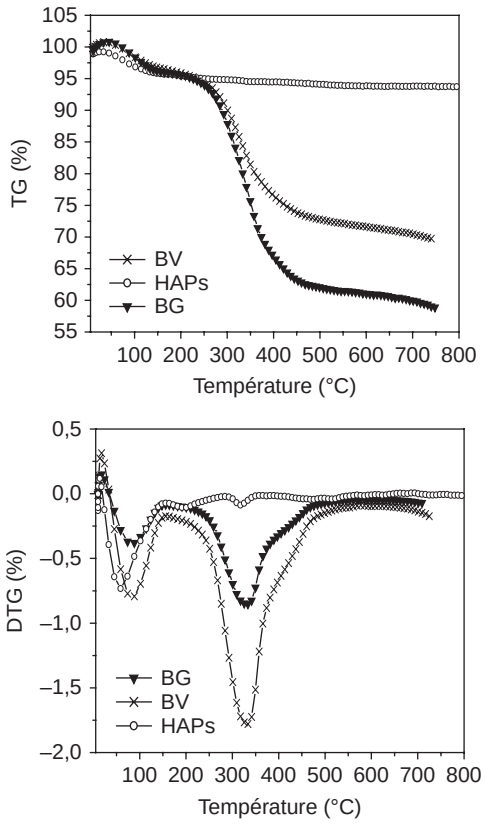

Fig. 1. TG and DTG pattern of (a) bovine bone (BV), (b) billy goat (BG) and (c) synthetic hydroxyapatite powder under nitrogen atmosphere.

was no significant weight loss between 600°C and 800°C, indicating that organic material such as fat tissues, collagen and proteins were completely removed. Annealing above 600°C, only the mineral phase (calcium phosphate) is left [25].

3.1.2. FTIR Analysis of BV, BG and HAPs

Fig. 2 represents the FT-IR characteristic results of HAPs, BV and BG. The FT-IR spectrum shows a number of absorption peaks, indicating the complex nature of waste bone. The bands at 3446 cm^{-1} representing bonded –OH groups [32]. Phosphate ions gave rise to two bands: a strong stretching band at 1041–1039 cm^{-1} and 600–603 cm^{-1}[33]. The bands observed at about 1450–1550 cm^{-1} could be assigned to the CO_3^{2-} group [34]. The peaks around 3560 cm^{-1} and 669 cm^{-1} correspond to the OH^- stretch [35]. In the case of the crude bovine and billy goat bones additional absorption peaks corresponding to a strong N-H stretching bond around 2921–2924 $cm^{-1}$and amide bands at 1540–1600 cm^{-1} were observed [36]. The two bands are characteristics of macromolecules of protein in the bovine and billy goat bone matrix. They disappeared when the bones were annealed at 600°C, indicating the complete removal of organic material.

3.1.3. XRD Analysis of BV, BG and HAPs

Fig. 3 represents the XRD pattern for the presence of nanocrystalline apatite in the bone matrixes. As the annealing temperature increased to 600°C (Fig. 3), the intensity of apatite-characterized peaks gradually increased indicating an increase in crystallinity and crystalline size. The XRD peaks obtained for the bovine bone and billy goat bone samples are having strong agreement with the characteristic peaks of HA pattern**.** The XRD pattern shows the position of three most prominent peaks position which corresponds to the plane (2 1 1), (3 0 0) and (2 0 2) of annealed bovine bone, billy goat bone and HAPs. In all cases, peak shifting was observed with 2θ values between 31.77° and 34.48°. These results indicated that in the animal bones dehydroxylaion of the hydroxyapatite has occurred during annealing [25].

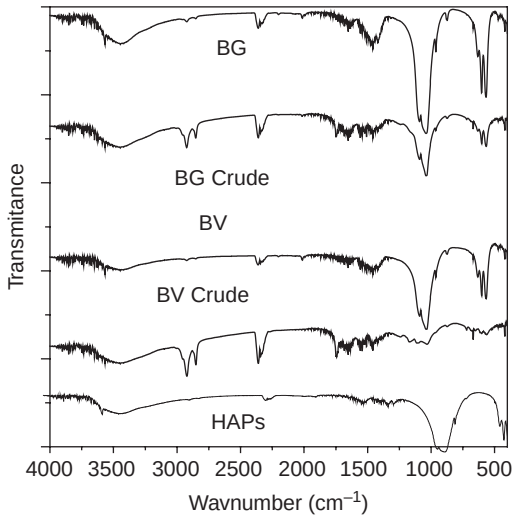

Fig. 2. FTIR spectra of bovine bone (BV), billy goat bone (BG) and synthetic hydroxyapatite powder (HAPs).

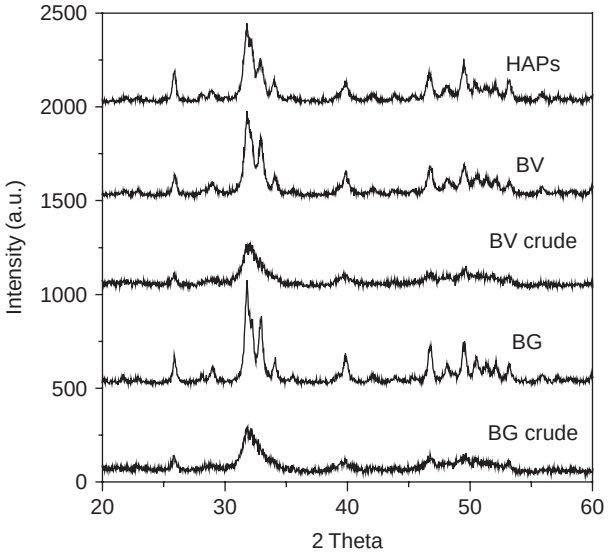

Fig. 3. XRD pattern of bovine bone (BV), billy goat bone (BG) and synthetic hydroxyapatite powder before and after calcinations.

3.2. Adsorption isotherm studies

The salient features of adsorption isotherms are needed before the kinetics of the adsorption process is interpreted. In order to investigate the sorption isotherm, five equilibrium models were analyzed: the Langmuir, Freundlich, Temkin, Elovich and Dubinin Raduskevich isotherm equations.

The Langmuir sorption isotherm is the best known of all isotherms describing sorption [30]. The Langmuir isotherm can be written to five linearized form: Eq. (6), Eq. (7), Eq. (8), Eq. (9), Eq. (10):

$$\frac{1}{q_e} = \frac{1}{q_m} + \frac{1}{K_L q_m C_e} \tag{6}$$

$$\frac{C_e}{q_e} = \frac{1}{q_m} C_e + \frac{1}{q_m K_L} \tag{7}$$

$$q_e = -\frac{1}{K_L}\frac{q_e}{C_e} + q_m \tag{8}$$

$$\frac{q_e}{C_e} = -K_L q_e + K_L q_m \quad (9)$$

$$\frac{1}{C_e} = K_L q_m \frac{1}{q_e} - K_L. \quad (10)$$

The values of the Langmuir constants K_L and q_m and the correlation coefficients are listed in Table 1 for BV, BG and HAPs.

From Table 1, it was observed that the values of Langmuir parameters obtained from the five linear expressions are different. It is clearly indicates that transformations of nonlinear model to linear forms alter their error structure and may also violate the error variance and normality assumptions of standard least-squares method [31]. The lower coefficient of correlation values for the Langmuir (1, 3, 4 and 5) linear expressions suggest that it is not appropriate to use this type of linearization. The values of maximum adsorption capacity were determined by using Langmuir-2 expression, which is higher than the experimental adsorbed amounts, and correspond to the adsorption isotherms plateaus. In contrast, the monolayer adsorption capacities obtained using Langmuir-1; Langmuir-3 and Langmuir-5 expressions are lower than the experimental values, which is unacceptable.

It is clearly indicates that the average percentage errors shown in Table 1 that the Langmuir-1, Langmuir-3, Langmuir-4 and Langmuir-5 expressions are unable to describe the equilibrium data for the majority of the studied adsorbents. In spite of the extremely higher coefficients of correlation obtained using Langmuir-1 and Langmuir-5 expressions, this model does not describe perfectly the equilibrium data because the higher values of average percentage error. Thus, it is not appropriate to use the coefficient of correlation of the linear regression method for comparing the best-fitting isotherms.

Table 1
Langmuir isotherm constants for the Zn(II) ion adsorption on bovine Bone (BV), billy goat bone (BG) and synthetic hydroxyapatite powder(HAPs).

Isotherms		BV	BG	HAPs
Langmuir-1	K_L(L mg^{-1})	0.094	0.203	1.655
	q_m(mg/g)	34.843	25.707	0.338
	R^2	0.975	0.726	0.929
	ARE (%)	18.56	27.46	65.99
	MPSD (%)	25.83	32.62	86.74
Langmuir-2	K_L(L mg^{-1})	0.185	0.226	0.049
	q_m(mg/g)	20.747	23.640	66.225
	R^2	0.981	0.887	0.309
	ARE (%)	9.65	19.16	20.66
	MPSD (%)	14.21	25.61	27.87
Langmuir-3	K_L(L mg^{-1})	0.239	0.609	0.364
	q_m(mg/g)	18.179	16.226	17.824
	R^2	0.719	0.339	0.086
	ARE (%)	13.70	26.24	42.97
	MPSD (%)	17.93	42.68	70.77
Langmuir-4	K_L(L mg^{-1})	0.172	0.207	0.032
	q_m(mg/g)	22.107	26.584	174.44
	R^2	0.719	0.339	0.086
	ARE (%)	10.99	21.70	22.14
	MPSD (%)	14.40	28.16	29.18
Langmuir-5	K_L(L mg^{-1})	0.077	0.026	1.264
	q_m(mg/g)	41.925	143.049	0.411
	R^2	0.975	0.726	0.929
	ARE (%)	22.71	51.49	96.57
	MPSD (%)	33.21	68.18	108.05

The Freundlich isotherm model was also used to explain the observed phenomena [37]:

$$\ln q_e = \ln K_F + n \ln C_e. \quad (11)$$

The Freundlich constant K_F and adsorption intensity 1/n for zinc(II) were calculated from the intercept and slop of the plot, the values are presented in Table 2. The correlation coefficient values are lower than the Langmuir value, which shows that the Langmuir equation represents a better fit of experimental data than the Freundlich equation.

Dubinin–Radushkevich (D-R) isotherm is based on the concept of energy and can be written as [38]:

$$\ln q_e = \ln q_m - \beta \left(\ln \left(1 + \frac{1}{C_e} \right) \right)^2, \quad (12)$$

where q_m is the maximum adsorption capacity (mol g^{-1}), and β is the constant related to the adsorption energy and the unit of C_e should be translated into mol L^{-1}. The mean free energy of the adsorption E is given by $E = (1/2\beta)^{0.5}$

This parameter gives information about the chemical or physical adsorption. The magnitude of E is between 8 and 16 kJ mol^{-1}, which represents chemical ion-exchange, while for the values of E < 8kJ mol^{-1} represnts that the biosorption process is physical in nature [38].

Temkin and Pyzhev [31] considered the effects of indirect adsorbate/adsorbate interactions on adsorption isotherms. They suggested that, because of these interactions and ignoring very low and very large values of concentration, the heat of adsorption of all molecules in the layer would decrease linearly with coverage:

$$q_e = B \ln A + B \ln Ce. \quad (13)$$

In Eq. (13), A and $RT/b = B$ are the Temkin isotherm constants. Constant B is related to the heat of adsorption.

The Elovich model was also used to study the kinetics of Zn(II) adsorption onto the three adsorbents. The equation is expressed as [37]:

$$\ln \frac{q_e}{C_e} = \ln K_E q_m - \frac{q_e}{q_m}. \quad (14)$$

In Eq. (14), K_E (L mg^{-1}) is the Elovich isotherm constant.

Table 2
Freundlich, Temkin, Elovich and Dubinin raduskevich isotherms constants for the adsorption of Zn (II) ion on BV, BG and HAPs.

Isotherms		BV	BG	HAPs
Freundlich	N	1.649	1.950	1.080
	K_F($mg^{(1-1/n)}$ $L^{1/n}$ g^{-1})	3.238	4.953	3.025
	R^2	0.927	0.807	0.907
	ARE (%)	15.87	19.42	25.40
	MPSD (%)	22.60	28.35	30.93
Temkin	A	2.324	2.648	1.367
	B	4.239	4.962	7.810
	R^2	0.989	0.894	0.992
	ARE (%)	11.12	21.16	12.62
	MPSD (%)	15.91	29.16	22.42
Elovich	K_E (L mg^{-1})	0.404	0.462	0.404
	q_m (mg g^{-1})	10.989	13.531	10.989
	R^2	0.817	0.501	0.817
	ARE (%)	16.49	29.70	52.94
	MPSD (%)	22.89	39.04	63.69
Dubminin	q_m(mol/g)	0.002	0.015	1.73
Raduskevich	B ($10^{-8}$$mol^2$ kJ^{-2})	0.4	0.4	5
	E (kJ mol^{-1})	11.18	11.18	3.162
	R^2	0.94	0.809	0.994
	ARE (%)	28.34	51.64	7.18
	MPSD (%)	20.97	34.25	4.13

From the Tables 1 and 2, it was observed that the model of Langmuir-2 is more suitable for the adsorption of Zn(II) on the BV and BG than that of the other model studied, and HAPs is more suitable for Dubinin model.

3.3. Kinetic study and diffusion model

The kinetics of adsorption that describes the solute uptake rate governing the residence time of the sorption reaction is one of the important characteristics that define the efficiency of sorption. Hence, in the present study, the kinetics of Zn(II) removal was carried out to understand the adsorption behavior of the prepared hydroxyapatite. Sorption of Zn(II) on hydroxyapatite involves a chemical sorption, which could control the reaction mechanism dissolution/precipitation. In order to investigate the mechanism of sorption, the rate constants of sorption and intraparticle diffusion model for the Zn(II) were determined using the equation of the pseudo-first-order, pseudo-second-order and the intra-particle diffusion model.

3.3.1. Pseudo-first-order kinetic model

The pseudo-first-order equation is given as [39]

$$\frac{dq_t}{dt} = K_1 \left(q_e - q_t\right), \tag{15}$$

where dq_t is the amount of Zn(II) adsorbed at time t (mg g^{-1}), q_e the adsorption capacity at equilibrium (mg g^{-1}), K_1 the pseudo-first-order rate constant (min^{-1}), and t the contact time (min). The integration of Eq. (15) with the initial condition, $q_t = 0$ at $t = 0$ leads to

$$\ln\left(q_e - q_t\right) = \ln q_e - K_1 t. \tag{16}$$

The values of the adsorption rate constant (K_1) for Zn(II) adsorption on BV, BG and HAPs were determined from the plot of $\ln(q_e - q_t)$ versus time t. A Zn(II) ion was assumed to adsorb on one sorption site of adsorbents (BV, BG and HAPs).

$$M\ (solid) + Zn^{2+} \rightarrow MZn^{2+}\ (adsorbed\ phase) \tag{17}$$

However from the Table 3 it was observed that (correlation coefficient and static's error) the pseudo-first-order equation is not suitable for the sorption of Zn(II) on the samples studied.

3.3.2. Pseudo-second-order kinetic model

The rate of pseudo-second-order reaction may be dependent on the amount of solute sorbed on the surface of adsorbent and the amount sorbed at equilibrium. The sorption equilibrium, q_e, is a function of, e.g., the initial metal ion concentration, the adsorbent dosage, the particle size, and the nature of solute–sorbent interaction.

The pseudo-second-order model is represented as [39]

$$\frac{dq_t}{dt} = K_2 \left(q_e - q_t\right)^2, \tag{18}$$

where K_2 is the pseudo-second-order rate constant. Integrating Eq. (20) the following equation is obtained:

$$\frac{t}{q} = \frac{1}{K_2 . q_e^2} + \frac{1}{q_e} . t. \tag{19}$$

Sorption of Zn(II) onto BV, BG and HAPs followed the pseudo-second-order kinetic model (Fig. 4). Consequently, the correlation coefficients calculated by using the pseudo-second-order model, i.e., R^2, and the pseudo-second-order parameters are shown in Table 4. From the Table 4, the linear regression analysis of the second-order rate equation showed higher R^2 value (0.9996). The rate constant K_2 was found to decrease with increasing of the concentration of Zn(II) (on the three adsorbents

Table 3
Pseudo-first-order kinetic model parameters for the adsorption of Zn(II) on the BV, BG and HAPs at 20°C.

Pseudo-first-order kinetic model	Parameters	Solute concentration (mg/L)			
		20	40	70	100
BV	K_1	1.064	4.499	2.858	4.275
	R^2	0.043	0.640	0.320	0.637
BG	K_1	4.346	3.508	3.522	3.563
	R^2	0.764	0.656	0.646	0.577
HAPs	K_1	4.617	4.094	3.827	4.426
	R^2	0.593	0.409	0.60	0.688

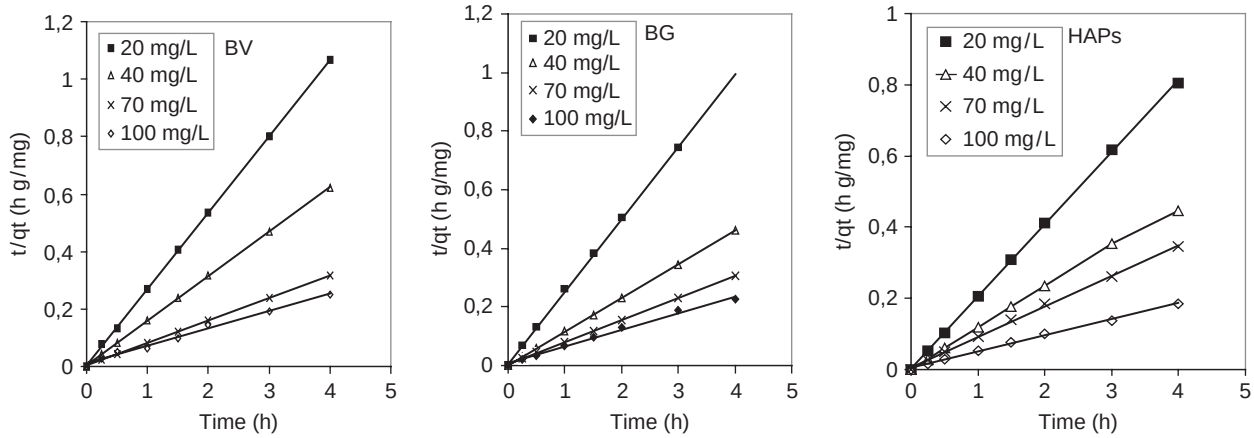

Fig. 4. Pseudo-second-order kinetic model for the adsorption of Zn(II) on the BV, BG and HAPs adsorbents (T = 20°C, ω = 250 rpm, pH = 5, C_{susp} = 5 g/L and time = 4 h).

Table 4
Pseudo-second-order parameters and standard deviations for the adsorption of Zn(II) on the BV, BG and HAPs at 20°C.

Pseudo-second order	Parameters	Solute concentration (mg/L)			
		20	40	70	100
BV	K_2	17.27	7.084	1.742	0.372
	R^2	0.999	0.999	0.999	0.991
	MPSD (%)	4.701	0.751	1.452	40.764
	ARE (%)	2.10	0.58	1.07	24.4 4
BG	K_2	12.021	9.413	2.044	0.411
	R^2	0.999	1	0.997	0.992
	MPSD (%)	1.745	0.66	4.490	4.553
	ARE (%)	1.24	0.39	2.43	4.08
HAPs	K_2	13.215	2.969	1.25	0.350
	R^2	0.999	0.998	0.999	0.997
	MPSD (%)	0.783	4.119	2.323	4.985
	ARE (%)	0.65	3.07	1.94	4.07

studied). It was observed that the solution with lower Zn(II) concentration is easy to equilibrate by the adsorbents BV, BG and HAPs. The results of pseudo-second-order kinetics found in this study are supported by the findings of many earlier works [40–41]. Sometimes there is a possibility that intraparticle diffusion will be the rate-limiting step.

3.3.3. Intraparticle diffusion model

The rate constant for the intraparticle diffusion (*Kp*) is given by Weber and Morris [40–42] as

$$q_t = K_p.t^{0.5} + C, \quad (20)$$

where K_p and C is intraparticle diffusion rate constant (mg/g $min^{0.5}$) and a constant, respectively. The intraparticle diffusion rate was obtained from the slope of the gentle-sloped portion of plot of q_t versus $t^{0.5}$. The intraparticle diffusion model considers the sorption as a three-stage process: the rapid adsorption, the gradual inward diffusion and the final equilibration. Fig. 5 shows the multi linearity of simulated curves for the tested data, which confirms these assumptions.

The adsorption process can be divided into three stages for solutions with initial concentrations, C_0 = 70 and 100 mg L^{-1}. However, the absence of the second linear portion was observed in solution with C_0 = 20 and 40 mg L^{-1}, indicating that the sorption was mainly surface adsorption. Table 5 represent the intraparticle diffusion rate parameters values for the adsorption of Zn(II) on different adsorbent, which was found that the K_{p1} value with HAPs is larger than that with BV and BG.

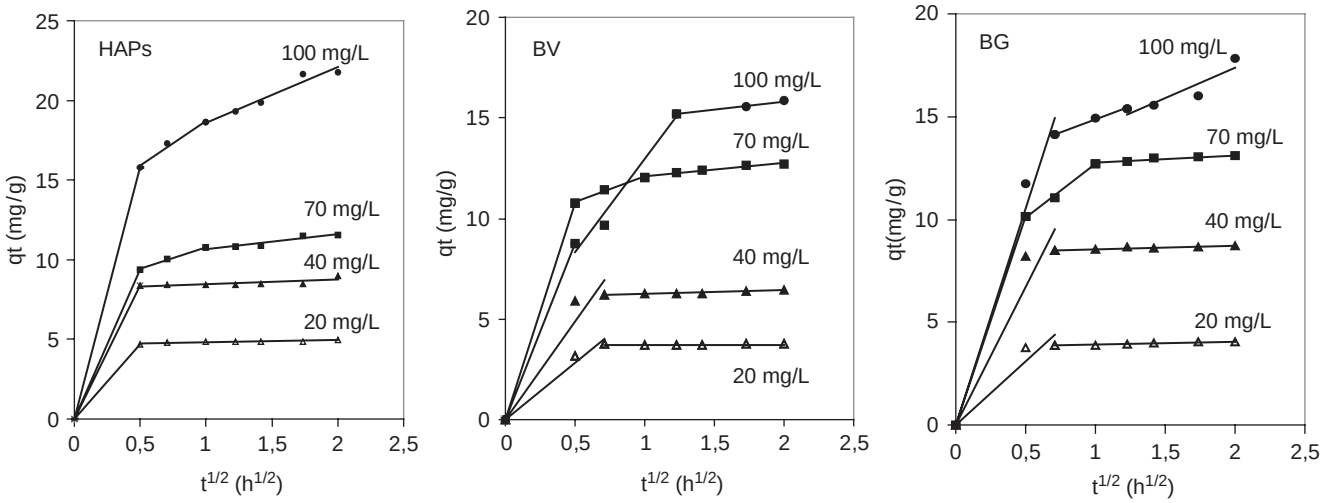

Fig. 5. Intraparticle diffusion model for the adsorption of Zn(II) on the BV, BG and HAPs adsorbents (T = 20°C, ω = 250 tr/min, pH = 5, C_{susp} = 5g/L and time = 4 h).

Table 5
Intraparticle diffusion parameters and standard deviations for the adsorption of Zn(II) on the BV, BG and HAPs at 20°C.

Intraparticle diffusion model	Parameters	Solute concentration (mg/L)			
		20	40	70	100
BV	K_{p1}	5.647	9.784	21.524	17.526
	K_{p2}	0.0104	0.169	2.530	9.273
	K_{p3}	–	–	0.648	0.815
	$(R_1)^2$	0.976	0.938	1	1
	$(R_2)^2$	0.126	0.918	0.986	0.976
	$(R_3)^2$	–	–	0.954	0.972
	MPSD (%)	4.615	6.954	0.447	8.673
	ARE (%)	2.04	3.16	0.36	5.3 2
BG	K_{p1}	6.1699	13.477	20.274	21.135
	K_{p2}	0.1572	0.1582	5.222	2.471
	K_{p3}	–	–	0.362	2.955
	$(R_1)^2$	0.927	0.931	1	0.982
	$(R_2)^2$	0.907	0.88	0.997	0.995
	$(R_3)^2$	–	–	0.915	0.838
	MPSD (%)	7.471	7.293	5.86	4.45
	ARE (%)	3.59	3.3	2.68	2.85
HAPs	K_{p1}	9.374	16.785	18.712	31.57
	K_{p2}	0.130	0.295	2.744	5.58
	K_{p3}	–	–	0.924	3.47
	$(R_1)^2$	1	1	1	1
	$(R_2)^2$	0.693	0.597	0.987	0.979
	$(R_3)^2$	–	–	0.893	0.949
	MPSD (%)	0.771	1.436	0.968	1.349
	ARE (%)	0.57	1.04	0.7	1.01

This is because HAPs has a larger external surface area for solute adsorption instantaneously. In contrast, the K_{p2} values with BV are larger than that with HAPs and BG, indicating that BV possesses more micropores for intraparticle diffusion. Based on the above discussions, the adsorption of Zn(II) on BV, BG and HAPs can be considered as the surface adsorption at low Zn(II) concentration (40 mgL^{-1}), and as the combination of surface

adsorption and pore-filling by diffusing at higher Zn(II) concentration. The results also demonstrated that the adsorption mechanism of the adsorbents studied follows pseudo-second-order kinetics with a significant contribution of intraparticle diffusion.

4. Conclusions

This study revealed that the natural hydroxyapatite is an effective biosorbent for the removal of Zn(II) from aqueous solution and was comparable to synthetic hydroxyapatite. Batch adsorption studies concluded that the amount of adsorption of Zn(II) on adsorbent is in the order of HAPs > BG > BV. The adsorption isotherm data obtained for the BV, BG and HAPs were treated according to Langmuir, Freundlich, Temkin, Elovich and Dubinin equations and the equilibrium data were best described by Langmuir-2 for BV and BG and Dubinin Raduskevich isotherm model for HAPs. Pseudo-second-order and intraparticle diffusion models can be used to characterize the kinetics of adsorption of the Zn(II) on the three samples. Mechanism analysis indicates that adsorption of Zn(II) by hydroxyapatite proceeds via a dissolution/precipitation processes including adsorption and ion-exchange.

Nomenclatures

BV	Bovine bone
BG	Billy goat bone
HAPs	Synthetic hydroxyapatite
K_L	Langmuir constant.
Ce	Equilibrium solute concentration in the aqueous phase (mg/L).
C_0	The initial concentration of the zinc in the bulk solution (mg/L).
K_F	Freundlich constant indicative of the relative adsorption capacity of the adsorbent ($mg^{1-1/n}.L^{1/n}.g^{-1}$).
K_E	Elovich equilibrium constant (L mg^{-1})
A and *B*	Temkin equilibrium constant.
E	Adsorption energy (kJ mol^{-1}).
B	Constant related to the adsorption energy (mol^2 kJ^{-2})
K_1	Pseudo- first-order rate constant of adsorption (min^{-1}).
K_2	Pseudo-second-order rate constant of adsorption (g mg^{-1} min^{-1}).
K_P	Intraparticle rate constant ($mg/g.min^{1/2}$).
M	Mass of adsorbent in the volume V (g).
N	Freundlich constant related to the intensity of the adsorption.
q_t	Amount of solute adsorbed by 1 g of the adsorbent at time t (mg/g).
q_e	Amount of solute adsorbed by 1 g of the adsorbent at the equilibrium concentration (mg/g).
q_m	Maximum adsorption capacity (mg/g).
R^2	Correlation coefficient.
T	Contact time (*h*).
V	Volume of the pollutant solution (L).
Y	Yield of adsorption (%).
C_{susp}	Concentration of the adsorbent (g/L).
Ω	Agitation (rpm).
T	Temperature (°C).
N	The number of experimental point.
q_{expi}	Experimental value of adsorbate concentration at equilibrium (mg/g).
q_{cali}	Calculated value of adsorbate concentration at equilibrium (mg/g).

References

[1] The Council of the European Communities, Directive 76/464/EEC–on pollution caused by certain dangerous substances discharged into the aquatic environment of the community, Off. J. Eur. Commun., (1976), No. L 129/23.

[2] J.G. Dean, F.L Bosqui, K.H Lanouette, Removing heavy metals from wastewater, Environ. Sci. Technol., 6 (1972) 518–522.

[3] M. Sitting, Handbook of Toxic and Hazardous Chemicals. Noyes Publications. Park Ridge. New Jersey, USA, 1981, 328.

[4] USDHHS, Toxicological Profile for Zinc, US Department of Health and Human Services, Agency for Toxic Substances and Disease Registry, Atlanta,, GA, 1993.

[5] L. Norton, K. Baskaran, S.T. McKenzie, Biosorption of zinc from aqueous solutions using biosolids, Adv. Environ. Res., 8 (2004) 629–635.

[6] C. Blöcher, J. Dorda, V. Mavrov, H. Chmiel, N.K. Lazaridis, K.A. Matis, Hybrid flotation—membrane filtration process for the removal of heavy metal ions from wastewater, Water. Res., 37 (2003) 4018–4026.

[7] N. Meunier, P. Drogui, C. Montané, R. Hausler, G. Mercier, J.F. Blais, Comparison between electrocoagulation and chemical precipitation for metals removal from acidic soil leachate, J. Hazard. Mater., 137 (2006) 581–590.

[8] B. Alyüz, S. Veli, Kinetics and equilibrium studies for the removal of nickel and zinc from aqueous solutions by ion exchange resins, J. Hazard. Mater., 167 (2009) 482–488.

[9] G. Borbély, E. Nagy, Removal of zinc and nickel ions by complexation–membrane filtration process from industrial wastewater, Desalination, 240 (2009) 218–226.

[10] S.K. Srivastava, V.K. Gupta, D. Mohan, Removal of lead and chromium by activated slag--A blast-furnace waste, J. Environ. Eng. (ASCE), 123 (1997) 461–468.

[11] V.K. Gupta, Equilibrium uptake, sorption dynamics, process development and column operations for the removal of copper and nickel from aqueous solution and wastewater using activated slag-a low cost adsorbent, Ind. Eng. Chem. Res. (ACS), 37 (1998) 192–202.

[12] V.K. Gupta, D. Mohan, S. Sharma, K.T. Park, Removal of chromium(VI) from electroplating industry wastewater using bagasse fly ash--A sugar industry waste material, Environmentalist, 19(2) (1999) 129–136.

[13] V.K. Gupta, C.K. Jain, I. Ali, S. Chandra, S. Agarwal, Removal of lindane and malathion from wastewater using bagasse fly ash–A sugar industry waste, Water Res., 36(10) (2002) 2483–2490.

[14] I. Ali, V.K. Gupta, Advances in water treatment by adsorption technology, Nat. Protoc., 1(6) (2007) 2661–2667.

[15] V.K. Gupta, I. Ali, V.K. Saini, Removal of fluoride from water by adsorption on carbon slurry: A waste material of fertilizer industry, Water Res., 41(15) (2007) 3317–3326.

[16] V.K. Gupta, I. Ali, Removal of endosulfan and methoxychlor from water on carbon slurry, Environ. Sci. Technol., 42 (2008) 766–770.
[17] S.R. Shukla, S.P. Roshan, Adsorption of Cu (II), Ni (II) and Zn (II) on dye loaded groundnut shells and sawdust, Sep. Purif. Technol., 43 (2005) 1–8.
[18] V.K. Gupta, M. Gupta, S. Sharma, Process development for the removal of lead and chromium from aqueous solutions using red mud–-An aluminium industry waste, Water Res., 35 (2001) 1125–1134.
[19] V.K. Gupta, C.K. Jain, I. Ali, M. Sharma, V.K. Saini, Removal of cadmium and nickel from wastewater using bagasse fly ash–A sugar industry waste, Water Res., 37 (2003) 4038–4044.
[20] V.K. Gupta, S. Sharma, Removal of zinc from aqueous solutions using bagasse fly ash—A low cost adsorbent, Ind. Eng. Chem. Res., 42 (2003) 6619–6624.
[21] V.K. Gupta, I. Ali, Removal of lead and chromium from wastewater using bagasse fly ash–-A sugar industry waste, J. Colloid Interface Sci., 271 (2004) 321–328.
[22] V.K. Gupta, A. Rastogi, V.K. Saini, N. Jain, Biosorption of copper (II) from aqueous solutions by algae spirogyra species, J. Colloid Interface Sci., 296 (2006) 53–60.
[23] V.K. Gupta, P.J.M. Carrott, M.M.L. Ribeiro Carrott, Suhas, Low cost adsorbents: Growing approach to wastewater treatment–A review, Crit. Rev. Environ. Sci. Technol., 39 (2009) 783–842.
[24] F. Banat, S. Al-Asheh, F. Mohai, Batch zinc removal from aqueous solution using dried animal bones, Sep. Purif. Technol., 21 (2000) 155–164.
[25] W. Admassu, T. Breese, Feasibility of using natural fish bone apatite as a substitute for hydroxyapatite in remediating aqueous heavy metals, J. Hazard. Mater., B69 (1999) 187–196.
[26] C.Y. Ooi, M. Hamdi, S. Ramesh, Properties of hydroxyapatite produced by annealing of bovine bone, Ceram. Int., 33 (2007) 1171–1177.
[27] A. Krestou, A. Xenidis, D. Panias, Mechanism of aqueous uranium(VI) uptake by hydroxyapatite, Miner. Eng., 17 (2004) 373–381.
[28] G. Lei, S. Chang-mei, L. Gui-ying, L. Chun-ping, J. Chun-nuan, Thermodynamics and kinetics of Zn(II) adsorption on cross linked starch phosphates, J. Hazard. Mater., 161 (2009) 510–515.
[29] Q.Y. Ma, S.J. Traina, T.J. Logan, J.A. Ryan, Effects of aqueous Al, Cd, Cu, Fe(II), Ni, and Zn on Pb immobilization by hydroxyapatite, Environ. Sci. Technol., 28 (1994) 1219–1228.
[30] E. Valsami-Jones, K.V. Ragnarsdottir, A. Putnis, D. Bosbach, A.J. Kemp, G. Cressey, The dissolution of apatite in the presence of aqueous metal cations at pH 2–7, Chem. Geol., 151 (1998) 215–233.
[31] E. Mavropoulos, A.M. Rossi, A.M. Costa, C.A.C. Perez, J.C. Moreira, M. Saldanha, Studies on the mechanisms of lead immobilization by hydroxyapatite, Environ. Sci. Technol., 36 (2002) 1625–1629.
[32] F. N. Arslanoglu, F. Kar, N. Arslan, Adsorption of dark coloured compounds from peach pulp by using powdered-activated carbon, J. Food. Eng., 71 (2005) 156–163.
[33] S. Joschek, B. Nies, R. Krotz, A. Gopferich, Chemical and physicochemical characterization of porous hydroxyapatite ceramics made of natural bone, Biomaterials, 21 (2000) 1645–1658.
[34] E. Landi, A. Tampieri, G. Celotti, R. Langenati, M. Sandri and S. Sprio, Nucleation of biomimetic apatite in synthetic body fluids: Dense and porous scaffold development, Biomaterials, 26 (2005) 2835–2848.
[35] A. Corami, S. Mignardi, V. Ferrini, Cadmium removal from single- and multi-metal (Cd+Pb+Zn+Cu) solutions by sorption on hydroxyapatite, J. Colloid. Interface Sci., 317 (2008) 402–408.
[36] B. Purevsuren, B. Avid, T. Gerelmaa, Ya. Davaajav, T.J. Morgan, A.A. Herod, R. Kandiyoti, The characterization of tar from the pyrolysis of animal bones, Fuel, 83 (2004) 799–805.
[37] S. Raynaud, E. Champion, D. Bernache-Assollant, P. Thomas, Calcium phosphate apatites with variable Ca/P atomic ratio I. Synthesis, characterization and thermal stability of powders, Biomaterials, 23 (2002) 1065–1072.
[38] O. Hamdaoui, E. Naffrechoux, Modeling of adsorption isotherms of phenol and chlorophenols onto granular activated carbon: Part I. Two-parameter models and equations allowing determination of thermodynamic parameters, J. Hazard. Mater., 147 (2007) 381–391.
[39] S.J. Allen, Q. Gan, R. Matthews, P.A. Johnson, Comparison of optimised isotherm models for basic dye adsorption by kudzu, Bioresour. Technol., 88 (2003) 143–152.
[40] S. Rengaraj, J.W. Yeon, Y. Kim, Y. Jung, H. Yeong-Keong, W.H. Kim, Adsorption characteristics of Cu(II) onto ion exchange resins 252H and 1500H: Kinetics, isotherms and error analysis, J. Hazard. Mater., 143 (2007) 469–477.
[41] S. Veli and B. Alyuz, Adsorption of copper and zinc from aqueous solutions by using natural clay, J. Hazard. Mater., 149 (2007) 226–233.
[42] M. Arshad, M. Nadeem Zafar, S. Younis, R. Nadeem, The use of Neem biomass for the biosorption of zinc from aqueous solutions, J. Hazard. Mater., 157 (2008) 534–540.